

# Photoproduction of light vector mesons in Xe-Xe ultraperipheral collisions at the LHC and the nuclear density of Xe-129

V. Guzey,<sup>1,2,3</sup> E. Kryshen,<sup>1</sup> and M. Zhalov<sup>1</sup>

<sup>1</sup>*National Research Center “Kurchatov Institute”,  
Petersburg Nuclear Physics Institute (PNPI), Gatchina, 188300, Russia*

<sup>2</sup>*Department of Physics, University of Jyväskylä,*

*P.O. Box 35, 40014 University of Jyväskylä, Finland*

<sup>3</sup>*Helsinki Institute of Physics, P.O. Box 64, 00014 University of Helsinki, Finland*

We make predictions for cross sections of  $\rho$  and  $\phi$  vector meson photoproduction in ultraperipheral Xe-Xe collisions at  $\sqrt{s_{NN}} = 5.44$  TeV. Analyzing the momentum transfer distribution of  $\rho$  mesons in this process, we explore the feasibility of extracting the nuclear density of  $^{129}\text{Xe}$ , which is needed in searches for dark matter with Xenon-based detectors.

## I. INTRODUCTION

Collisions of ultrarelativistic ions at large impact parameters – the so-called ultraperipheral collisions (UPCs) – provide opportunities to explore photon–photon, photon–proton, and photon–nucleus interactions at previously unattainable high energies [1]. In particular, a test run of collisions of Xenon ions was performed at the Large Hadron Collider (LHC) in Fall 2017. The experiments have collected several  $\mu\text{b}^{-1}$  of statistics, which is sufficient to study photoproduction of light  $\rho$  and  $\phi$  vector mesons. Extending the formalism [2], which reasonably describes coherent  $\rho$  meson photoproduction in Au-Au UPCs [3] at the Relativistic Heavy Ion Collider (RHIC) and Pb-Pb UPCs [4] at the LHC, we consider coherent and incoherent  $\rho$  and  $\phi$  meson photoproduction in Xe-Xe UPCs in the LHC kinematics at  $\sqrt{s_{NN}} = 5.44$  TeV and predict the corresponding UPC cross sections as functions of the vector meson rapidity  $y$  and the momentum transfer  $t$ . These predictions combined with the earlier results for Pb-Pb UPCs provide the nuclear mass number  $A$  dependence of our approach to nuclear shadowing in light vector meson photoproduction on nuclei and can be compared to the future LHC data.

In the past, based on the vector meson dominance (VMD) model, photoproduction of light vector mesons on nuclei was used to determine the meson–nucleon cross section and to constrain the nuclear matter density distribution of the target [5]. To our knowledge, only the root-mean-square (rms) charge radii of Xe isotopes have been extracted from isotope shift measurements [6] and the charge density distribution of  $^{132}\text{Xe}$  was recently determined [7] from electron-xenon elastic scattering at SCRIT facility. At the same time the nuclear matter distribution, the effective nuclear radius, and the structure factors of Xe isotopes are of key importance for Dark Matter experiments searching for weakly interacting massive particles (WIMP) with Xenon-based detectors (for details, see, e.g. [8–10]). In this note we demonstrate that the measurement of  $\rho$  photoproduction in Xe-Xe UPC at the LHC can be used to gain information on the nuclear matter distribution in  $^{129}\text{Xe}$ .

## II. COHERENT AND INCOHERENT CROSS SECTIONS OF $\rho$ AND $\phi$ PHOTOPRODUCTION IN NUCLEUS–NUCLEUS UPCS

The cross section of coherent and incoherent (the target nucleus breaks up) cross section of vector meson  $V$  ( $V = \rho, \phi$ ) photoproduction in symmetric nucleus–nucleus UPCs reads [1]:

$$\frac{d\sigma_{AA \rightarrow VAA'}(y)}{dy} = N_{\gamma/A}(y)\sigma_{\gamma A \rightarrow VA'}(y) + N_{\gamma/A}(-y)\sigma_{\gamma A \rightarrow VA'}(-y), \quad (1)$$

where  $N_{\gamma/A}$  is the photon flux;  $y$  is the rapidity of the produced vector meson  $V$ ;  $\sigma_{\gamma A \rightarrow VA'}(y)$  is the photoproduction cross section. The target nucleus label  $A'$  stands for both coherent  $A' = A$  and incoherent  $A' \neq A$  cases. The presence of two terms with the opposite rapidities in Eq. (1) reflects the fact that each colliding ion can serve as a source of photons and as a target.

The photon flux  $N_{\gamma/A}(y)$  produced by an ultrarelativistic ion in nucleus–nucleus UPCs in Eq. (1) can be very well approximated by the photon flux due to a point-like charge  $Z$ :

$$N_{\gamma/A}(y) = \frac{2Z^2\alpha_{\text{e.m.}}}{\pi} \left[ \zeta K_0(\zeta)K_1(\zeta) - \frac{\zeta^2}{2} (K_1^2(\zeta) - K_0^2(\zeta)) \right], \quad (2)$$

where  $\alpha_{\text{e.m.}}$  is the fine-structure constant;  $K_{0,1}$  are Bessel functions of the second kind;  $\zeta = \omega b_{\text{min}}/\gamma_L$ ;  $\omega = (M_V/2)e^y$  is the photon energy for given  $y$ , where  $M_V$  is the vector meson mass;  $\gamma_L$  is the nucleus Lorentz factor in the laboratory frame;  $b_{\text{min}}$  is the minimal transverse distance between the centers of the colliding nuclei specifying the ultraperipheral collision. Its value  $b_{\text{min}} \approx 2R_A$  ( $R_A$  is the radius of the nucleus) is found by requiring that Eq. (2) reproduces the photon flux, which is calculated as convolution over impact parameters of the flux of equivalent photons produced by the charge distribution of the radiating nucleus with the probability to not have the strong inelastic interactions in a given nucleus–nucleus collision.

In high-energy UPCs of heavy ions with the large charge  $Z$ , the photoproduction process can be accompanied by additional photon exchanges between colliding ions because the parameter  $\alpha_{\text{e.m.}}^2 Z^2$  is not small. These additional photon exchanges may lead to excitations of one or both colliding nuclei [11, 12], which typically decay by emission of one or more neutrons moving along the direction of ion beams and detected by zero-degree calorimeters (ZDCs). The low-energy electromagnetic excitation of nuclei and the high-energy vector meson photoproduction in UPC can be considered as independent processes because of the large difference in time scales. Hence, one can account for the additional photon exchanges by modifying the photon flux and, thus, selecting photoproduction of vector mesons in nucleus–nucleus UPCs in different channels  $i$ , which are specified by emission of various number of neutrons  $i = (0n0n, 1n1n, 0nXn, XnXn, \dots)$  [13]. In particular, the photon flux for channel  $i$  reads:

$$N_{\gamma/A}^i(y) = \int_{2R_A}^{\infty} d^2\vec{b} N_{\gamma/A}(y, \vec{b}) P_i(\vec{b}) \quad (3)$$

where  $N_{\gamma/A}(y, \vec{b})$  is the photon flux at the transverse distance  $b$  (impact parameter) from the center of the nucleus, which produces it;  $P_i(\vec{b})$  is the probability to emit a given number of neutrons corresponding to channel  $i$ . This approach describes very well the ALICE data on electromagnetic dissociation in Pb–Pb UPCs [14] and is implemented in the Starlight Monte Carlo generator [15], which is commonly used for calculations and simulations of various UPC processes. Note that an alternative approach to electromagnetic excitation of nuclei with neutron emission in UPCs, which is based on the Hauser–Feshbach formalism and which provides a good description of the RHIC and LHC data on electromagnetic excitations in UPCs, was developed in [16].

The coherent  $\gamma A \rightarrow VA$  cross section  $\sigma_{\gamma A \rightarrow \rho A}$  in Eq. (1) can be calculated using the combination of the Gribov–Glauber model for nuclear shadowing and a model for hadronic fluctuations for the  $\gamma N \rightarrow VN$  cross section [2, 17]. This approach provides a good description of the data on coherent  $\rho$  photoproduction on heavy nuclei in UPCs at RHIC and the LHC (Run 1). It is based on the observation that at high energies, the real photon interacts with hadronic targets by means of its long-lived hadronic components (fluctuations). Each fluctuation is characterized by the cross section  $\sigma$  and interacts independently with nucleons of a nuclear target; the probability distribution of these fluctuations  $P(\sigma)$  is constrained using the experimental data on the elastic  $\gamma p \rightarrow Vp$  and the diffraction dissociation  $\gamma p \rightarrow Xp$  cross sections, see details in Ref. [2, 18]. Thus, the  $\gamma A \rightarrow VA$  cross section in the large  $W_{\gamma N}$ -limit ( $W_{\gamma N}$  is the invariant photon–nucleus energy per nucleon) is given by the following expression:

$$\sigma_{\gamma A \rightarrow VA}^{\text{mVMD-GGM}}(W_{\gamma N}) = \left( \frac{e}{f_V} \right)^2 \int d^2\vec{b} \left| \int d\sigma P(\sigma) \left( 1 - e^{-\frac{\sigma}{2} \tilde{T}_A(\vec{b})} \right) \right|^2, \quad (4)$$

where  $f_V$  is the  $\gamma - V$  coupling constant ( $f_\rho^2/4\pi = 2.01$  for  $\rho$  and  $f_\phi^2/4\pi = 13.7$  for  $\phi$ );  $\tilde{T}_A(\vec{b}) = \int_{-\infty}^{\infty} dz \rho_A(\vec{b}, z) - (l_c \sigma)/2 \int_{-\infty}^{\infty} dz \rho_A^2(\vec{b}, z)$  is the nuclear optical density, which also takes into account short-range nucleon–nucleon ( $NN$ ) correlations in the nuclear wave function, where  $\rho_A(b, z)$  is the nuclear density and  $l_c = -0.74$  fm is the  $NN$  correlation length. For lower values of  $W_{\gamma N} \leq \mathcal{O}(\sqrt{2R_A m_N M_V}) \approx 5$  GeV, the expression in Eq. (4) should be corrected by including the effects of the non-zero longitudinal momentum transfer in the  $\gamma N \rightarrow VN$  amplitude (the effect of nuclear coherence). It suppresses the  $d\sigma_{AA \rightarrow VAA}/dy$  UPC cross section (1) at forward and backward rapidities but does not affect it near  $y \approx 0$ .

In the case of incoherent nuclear scattering, the  $\gamma A \rightarrow VA'$  quasi-elastic cross section  $\sigma_{\gamma A \rightarrow \rho A'}$  can be calculated using completeness of final nuclear states  $A'$ , see, e.g. [5]. Applying the photon fluctuations to the nuclear scattering amplitudes, one obtains:

$$\sigma_{\gamma A \rightarrow VA'}^{\text{mVMD-GGM}}(W_{\gamma N}) = \sigma_{\gamma N \rightarrow VN}(W_{\gamma N}) \int d^2\vec{b} \tilde{T}_A(\vec{b}) \left| \int d\sigma P(\sigma) \frac{\sigma}{\langle \sigma \rangle} e^{-\frac{\sigma}{2} \tilde{T}_A(\vec{b})} \right|^2, \quad (5)$$

where  $\langle \sigma \rangle = \int d\sigma P(\sigma) \sigma$ . Equation (5) has a clear physical interpretation: quasi-elastic photoproduction of  $\rho$  mesons on a nuclear target corresponds to elastic  $\rho$  production on any from all  $A$  target nucleons with the condition that interactions with remaining nucleons do not lead to inelastic production. The probability to not have inelastic

processes describes the effect of nuclear shadowing for individual fluctuations and depends on the distribution  $P(\sigma)$ . In the absence of fluctuations, it reduces to the familiar Glauber model expression.

In collider kinematics of ion UPCs at ALICE, it is problematic to separate the quasielastic incoherent process  $\gamma A \rightarrow VA'$  and photoproduction of vector mesons  $\gamma A \rightarrow VA'Y$  with nucleon dissociation  $\gamma N \rightarrow VY$  into not too large masses  $M_Y < 10$  GeV. All fragments  $Y$  are going in the very forward direction along the beams. We estimate the contribution of this process within the Gribov–Glauber model. In particular, an examination of corresponding multiple scattering graphs shows that the  $\gamma N \rightarrow VY$  cross section  $\sigma_{\gamma N \rightarrow VY}$  factorizes out and the remaining nuclear shadowing suppression is the same as in the case of Eq. (5). It can also be shown formally by generalizing the derivation of Eq. (5) to include color fluctuations [19] in target nucleons (nucleon shape fluctuations [20]) and keeping the leading power of the variance of these fluctuations. To this accuracy, the form of these fluctuations is not important; the variance is expressed in terms of  $d\sigma_{\gamma N \rightarrow VY}(t=0)/dt$ . Therefore, the incoherent cross section of light vector meson  $V$  photoproduction on nuclei with target nucleon dissociation is given by the following expression:

$$\sigma_{\gamma A \rightarrow VA'Y}^{\text{mVMD-GGM}}(W_{\gamma N}) = \sigma_{\gamma N \rightarrow VY}(W_{\gamma N}) \int d^2\vec{b} T_A(\vec{b}) \left| \int d\sigma P(\sigma) \frac{\sigma}{\langle \sigma \rangle} e^{-\frac{\sigma}{2} \bar{T}_A(\vec{b})} \right|^2. \quad (6)$$

Calculations of the cross section of  $\rho$  photoproduction with dissociation of the proton target in the non-perturbative domain of small values of  $|t|$  are strongly model-dependent. Instead, for the kinematical region of ALICE measurements, we use the HERA results [21, 22] and obtain for the ratio of the forward target-dissociative and elastic  $\rho$  photoproduction cross sections on the proton:

$$\frac{d\sigma_{\gamma p \rightarrow \rho Y}(t \approx 0)/dt}{d\sigma_{\gamma p \rightarrow \rho p}(t \approx 0)/dt} \approx 0.1 - 0.12. \quad (7)$$

Combining this value with the ratio of corresponding slope parameters of the  $t$  dependence  $B_{\text{diss}}/B_{\text{el}} \approx 0.25$  (it is assumed that the  $t$  dependence is exponential), we obtain the following relation:

$$\sigma_{\gamma p \rightarrow VY}(W_{\gamma p}) \approx 0.5 \sigma_{\gamma p \rightarrow Vp}(W_{\gamma p}). \quad (8)$$

Note that this relation also agrees very well with the ratio of the elastic and proton-dissociation cross sections of  $\rho$  electroproduction in a wide range of  $Q^2$  and at  $W_{\gamma p} = 75$  GeV measured by the H1 collaboration at HERA [23], which shows that Eq. (8) is approximately  $Q^2$ -independent.

It should be emphasized that the  $t$ -integrated cross section of vector meson photoproduction with target nucleon dissociation is comparable with the incoherent quasielastic cross section due to the contribution of large  $|t|$  and a smaller slope parameter. The contribution of this process in the case of a heavy nuclear target is not essential for small  $|t|$ , in particular, in the region  $|t| < 0.02$  GeV<sup>2</sup>, where coherent photoproduction dominates the momentum transfer distribution.

Before discussing results of our calculations presented in Figs. 1-4, we note that the detailed description of our approach, the modified VMD-GGM, is given in [2]. Here we only emphasized the feature specific for the current calculations. The main part of our results is obtained with the nuclear matter density distribution of  $^{129}\text{Xe}$  calculated within the standard spherical Hartree–Fock–SkyrmeIII model with accounting for the BCS pairing (no special fit specific to the Xe nucleus was done). This model gives the values of rms mass radius of  $^{129}\text{Xe}$  equal to 4.818 fm and the charge rms radius equal to 4.77 fm. The latter can be compared to the experimental value  $4.7831 \pm 0.0043$  [6] obtained from the isotope shift measurements. The effective radius  $R_A = 5.8$  fm, which is determined as the distance from the center to the point, where the mass density decreases by a factor of two compared to its maximal value, is somewhat larger than the value  $R_A = 5.45$  fm, which is given by the commonly used parametrization  $R_A = 1.112 A^{1/3} - 0.86 A^{-1/3}$  fm.

### III. RESULTS

The calculated rapidity distributions for  $\rho$  and  $\phi$  mesons produced in ultraperipheral Xe-Xe collisions at  $\sqrt{s_{NN}} = 5.44$  TeV are presented in Figs. 1 and 2, respectively. In four panels we show the total rapidity distribution and the rapidity distributions in different channels: “0n0n” is the case without additional photon exchanges, whose experimental signature is no neutrons detected in zero-degree calorimeters (ZDCs), the “0nXn” channel corresponds to electromagnetic excitation with subsequent neutron decay of only one of colliding ions, and “XnXn” is the case of mutual excitation of both ions. Red solid lines with strips show the coherent cross section with the uncertainty of our model in accounting for Gribov inelastic shadowing. Blue dashed lines show the contribution to the rapidity distribution from one target nucleus corresponding to the first term in Eq. (1). Finally, the black dot-dashed line

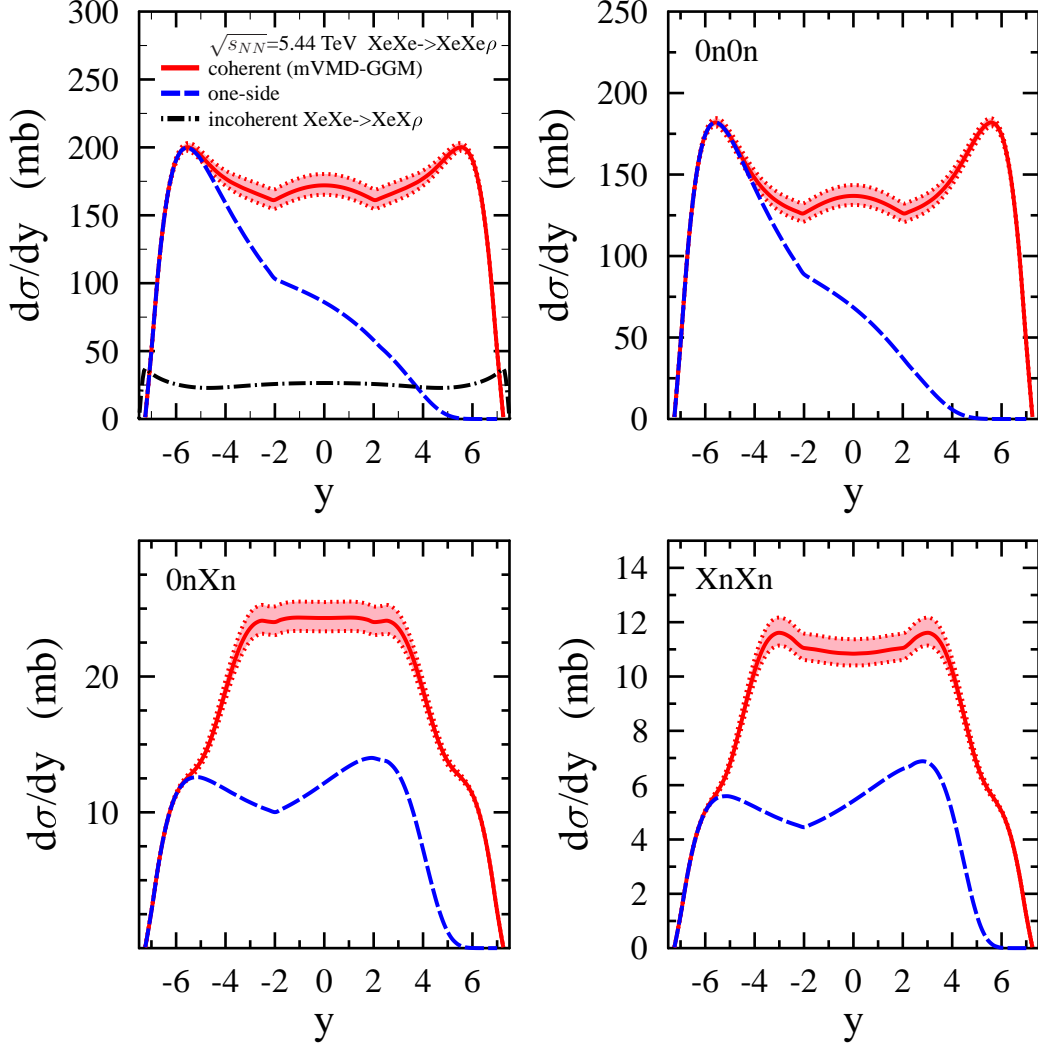


FIG. 1: Rapidity distributions for  $\rho$  photoproduction in ultraperipheral Xe-Xe collisions at  $\sqrt{s_{NN}} = 5.44$  TeV at the LHC. See explanations in text.

presents the summed contribution of quasielastic and nucleon target-dissociative photoproduction calculated as described above. Specifically, the black dot-dashed line is obtained by adding the contributions of Eqs. (5) and (6), where the proton-dissociation cross section  $\sigma_{\gamma p \rightarrow VY}(W_{\gamma p})$  is calculated using Eq. (8). As one can see from Eq. (8), the inclusion of the proton dissociation contribution increases the  $t$ -integrated nuclear incoherent cross section by approximately 50%. All cross sections in Figs. 1 and 2 have been integrated over the momentum transfer.

The shape of the rapidity distributions for coherent photoproduction reflects an interplay of several phenomena. Bumps at forward and backward rapidities in upper panels of Fig. 1 are due to an enhanced contribution of low-energy photoproduction related to the secondary Reggeon exchange in the  $\rho$ -N interaction; the inelastic Gribov shadowing at low energies is still small. Since only the Pomeron exchange contributes to the  $\phi$ -N interaction, such bumps are absent in  $\phi$  photoproduction (Fig. 2). The one-side contribution demonstrates how an interplay of the energy dependence of the elementary cross section, suppression due to nuclear shadowing, and drop of the flux of high-energy equivalent photons determine the distribution in the central and forward rapidity regions. A comparison of the distributions in different channels shows that additional photon exchanges resulting in neutron decays of excited nuclei enhance the role of smaller impact parameters of the collision [13] and, correspondingly, enhance the high-energy contribution to

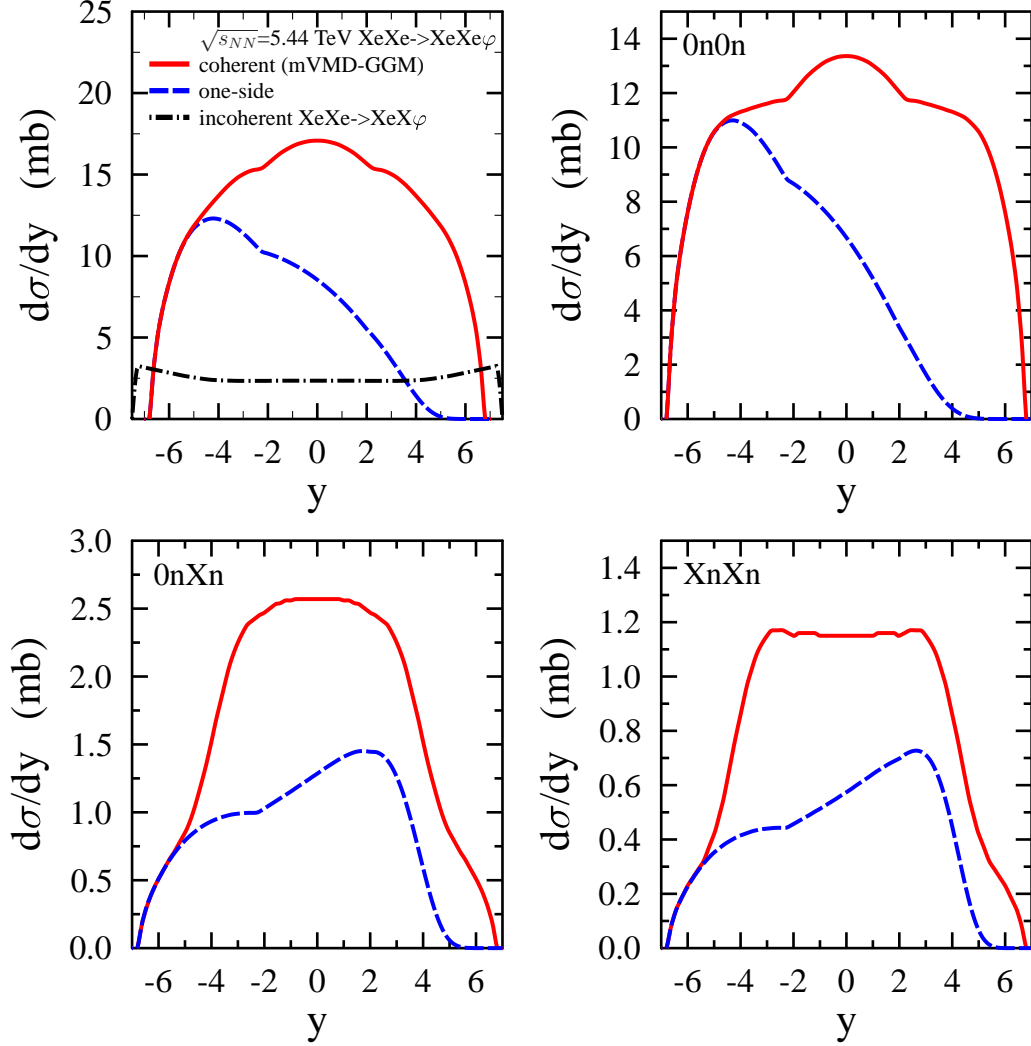


FIG. 2: Rapidity distributions for  $\phi$  photoproduction in ultraperipheral Xe-Xe collisions at  $\sqrt{s_{NN}} = 5.44$  TeV at the LHC. See explanations in text.

the UPC cross section.

The calculated transverse momentum distributions at the rapidity  $y = 0$  are presented in Fig. 3. The coherent cross section is shown by the red dashed line, the incoherent one – by the blue dotted line, and the summed cross section is given by the solid black curve. Here we neglected the contribution of the photoproduction process with nucleon dissociation, whose contribution is at the level of a few percent in the region of small  $|t| < 0.1$  GeV<sup>2</sup>. We also neglected washing out of the diffractive dip in the coherent cross section due to a small, but non-vanishing transverse momentum of quasireal photons [24] and the real part of the meson–nucleon amplitude.

It is well known that the position of diffractive dips is very sensitive to the radius of the target nucleus. Hence, to reveal them more clearly one needs to suppress the incoherent contribution. It can be achieved by selecting the “0n0n” channel of photoproduction, where one requires no forward neutron emission. It was shown in [25] that incoherent events of high energy photoproduction of vector mesons for  $|t| > 0.03$  GeV<sup>2</sup> are predominantly accompanied by neutrons from the decay of the excited residual nucleus. In Fig. 4 we show the momentum transfer distributions for the “0n0n” channel in photoproduction of  $\rho$  meson in Xe-Xe UPCs at the rapidity  $y = 0$ . To reveal the possibility of study the influence of the nuclear radius, we performed these calculations with the two-parameter Fermi distribution

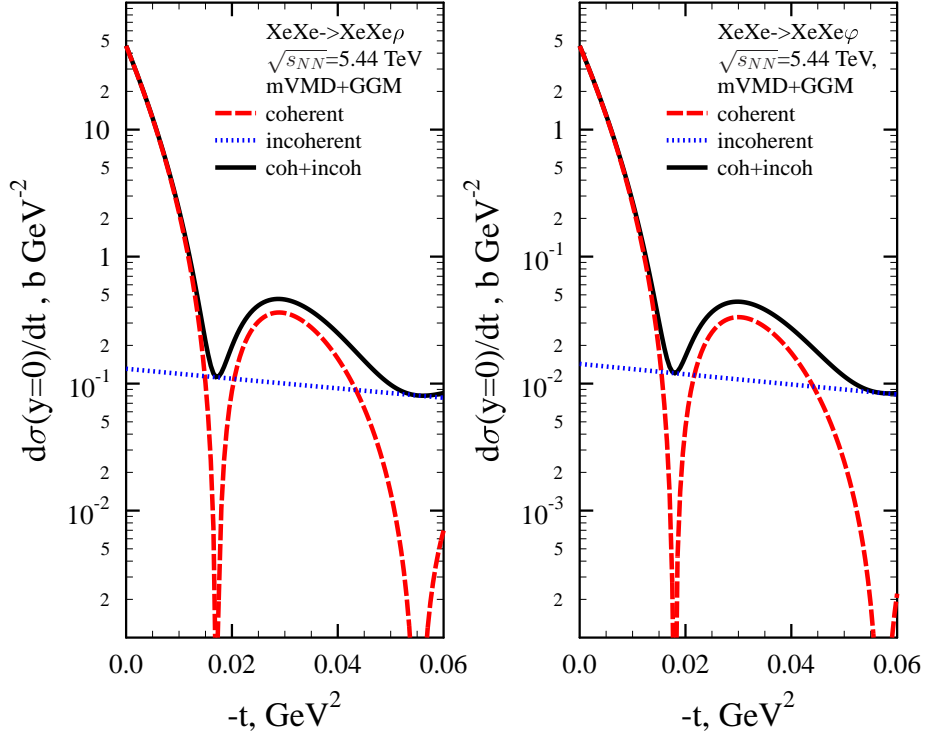


FIG. 3: The  $t$ -dependence of cross section of light vector meson ( $\rho$  on the left and  $\phi$  on the right) photoproduction in ultraperipheral Xe-Xe collisions at the LHC at  $\sqrt{s_{NN}} = 5.44$  TeV.

of the nuclear density  $\rho(r) = \rho_0[1 + \exp((r - R_A)/a)]^{-1}$  with the parameters  $a = 0.54$  and  $R_A = 6.1$  fm and with  $R_A = 5.45$  fm. It is seen that in measurements with high statistics and momentum resolution, by fitting the shape of the momentum transfer distribution in the region up to  $|t| \approx 0.1$  GeV<sup>2</sup>, one can determine the nuclear radius with rather high accuracy. Note that the theoretical uncertainty of our calculation of inelastic nuclear shadowing, which is shown by shaded bands in Fig. 1, affects primarily the cross section magnitude and not the shape of the  $t$  dependence. Hence, this theoretical uncertainty does not affect positions of the minima in Figs. 3 and 4.

There are also alternative approaches to calculation of light vector meson photoproduction in UPCs, notably, the one based on the color dipole framework and the phenomenological data-driven approach, which is used in Starlight Monte-Carlo generator. Briefly, photoproduction of light vector mesons in heavy ion Pb-Pb UPCs at the LHC has been extensively studied in the framework of the color dipole model including saturation effects [26–29]. Since the cross section of the discussed process is very sensitive to the non-perturbative contribution of large dipoles, the dipole model predictions strongly depend on the choice of the dipole cross section in this region and the final light vector meson wave function. In addition, due to the sub-leading Reggeon contribution to the  $\gamma p \rightarrow \rho p$  cross section, we predict a two-bump shape of the rapidity distribution  $d\sigma_{AA \rightarrow \rho AA}/dy$ , while the dipole models naturally lead to the distribution, which is bell-shaped.

Another framework to describe photoproduction of vector mesons in ion UPCs is based on the Starlight Monte-Carlo generator [15]. It combines phenomenological parameterizations of the  $\gamma p \rightarrow Vp$  cross sections on the proton with the optical theorem and the classical expression for the interaction of vector mesons with nuclei and rather successfully describes the available data on  $\rho$  photoproduction in Au-Au UPCs at RHIC and Pb-Pb UPCs at the LHC [30, 31]. In the context of present analysis, it is important to note that while the  $t$  dependence of  $d\sigma_{\gamma A \rightarrow VA}/dt$

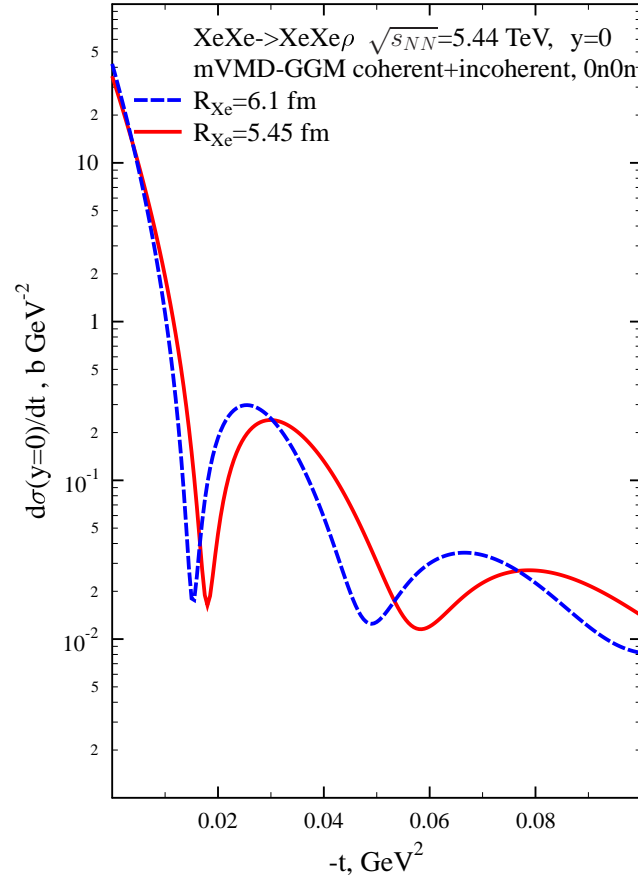


FIG. 4: The momentum transfer distribution of  $\rho$  photoproduction in Xe-Xe UPCs calculated using the mVMD-GGM approach with the two-parameter Fermi distribution of the Xenon nuclear density and two values of  $^{129}\text{Xe}$  radius.

is given by the nuclear form factor squared  $F_A^2(t)$  in Starlight (which is true in the limit of small nuclear shadowing), it is shifted towards smaller  $|t|$  in our case. An indication of this trend is seen in the ALICE data on coherent  $\rho$  photoproduction in Pb-Pb UPCs at  $\sqrt{s_{NN}} = 2.76$  TeV [4]. For further critical discussion of treatment of light vector meson photoproduction in ion UPCs using the color dipole model and Starlight Monte-Carlo generator, see Ref. [2].

One should note that the short Xe-Xe run did not allow one to collect high enough statistics of events with photoproduction of quarkonia in Xe-Xe UPCs. At the same time, studies of coherent photoproduction of vector mesons interacting with nuclear medium with different strengths should be very informative for the precise determination of nuclear density parameters from the transverse momentum distribution. In particular, the position of the dips depends on the strength of absorption of the produced mesons by the nucleus. We plan to perform in the near future such an analysis for nuclear targets of interest in light of future experiments at a planned electron-ion collider.

## IV. CONCLUSION

In this paper we presented our predictions for photoproduction of light vector mesons in ultraperipheral Xe-Xe collisions at the LHC. We showed that the analysis of the data on this process will provide useful information on nuclear shadowing, in particular, on the nuclear mass number  $A$  dependence of nuclear shadowing in light vector meson photoproduction on nuclei. We argue that the measured momentum transfer distributions can be used to gain new information on the density distribution of nuclear matter in  $^{129}\text{Xe}$  and, hence, to constrain the elastic form factor of this nucleus, which is essential in the search for WIMP with Xenon-based detectors.

- 
- [1] A. J. Baltz *et al.*, Phys. Rept. **458**, 1 (2008) [arXiv:0706.3356 [nucl-ex]].
  - [2] L. Frankfurt, V. Guzey, M. Strikman and M. Zhalov, Phys. Lett. B **752**, 51 (2016) [arXiv:1506.07150 [hep-ph]].
  - [3] C. Adler *et al.* [STAR Collaboration], Phys. Rev. Lett. **89**, 272302 (2002) doi:10.1103/PhysRevLett.89.272302 [nucl-ex/0206004].
  - [4] J. Adam *et al.* [ALICE Collaboration], JHEP **1509**, 095 (2015) doi:10.1007/JHEP09(2015)095 [arXiv:1503.09177 [nucl-ex]].
  - [5] T. H. Bauer, R. D. Spital, D. R. Yennie and F. M. Pipkin, Rev. Mod. Phys. **50**, 261 (1978) Erratum: [Rev. Mod. Phys. **51**, 407 (1979)].
  - [6] J. Libert, B. Roussire and J. Sauvage, Nucl. Phys. A **786**, 47 (2007).
  - [7] K. Tsukada *et al.*, Phys. Rev. Lett. **118**, no. 26, 262501 (2017) [arXiv:1703.04278 [nucl-ex]].
  - [8] H. Uchida *et al.* [XMASS-I Collaboration], PTEP **2014**, no. 6, 063C01 (2014) [arXiv:1401.4737 [astro-ph.CO]].
  - [9] L. Vietze, P. Klos, J. Menndez, W. C. Haxton and A. Schwenk, Phys. Rev. D **91**, no. 4, 043520 (2015) [arXiv:1412.6091 [nucl-th]].
  - [10] A. Fieguth, M. Hoferichter, P. Klos, J. Menndez, A. Schwenk and C. Weinheimer, arXiv:1802.04294 [hep-ph].
  - [11] M. Vidovic, M. Greiner and G. Soff, Phys. Rev. C **48** (1993) 2011.
  - [12] I. A. Pshenichnov, J. P. Bondorf, I. N. Mishustin, A. Ventura and S. Masetti, Phys. Rev. C **64** (2001) 024903 [nucl-th/0101035].
  - [13] A. J. Baltz, S. R. Klein and J. Nystrand, Phys. Rev. Lett. **89**, 012301 (2002) [nucl-th/0205031].
  - [14] B. Abelev *et al.* [ALICE Collaboration], Phys. Rev. Lett. **109** (2012) 252302 [arXiv:1203.2436 [nucl-ex]].
  - [15] S. R. Klein, J. Nystrand, J. Seger, Y. Gorbunov and J. Butterworth, Comput. Phys. Commun. **212** (2017) 258 [arXiv:1607.03838 [hep-ph]].
  - [16] M. Klusek-Gawenda, M. Ciemala, W. Schafer and A. Szczurek, Phys. Rev. C **89** (2014) no.5, 054907 [arXiv:1311.1938 [nucl-th]].
  - [17] V. Guzey, M. Strikman and M. Zhalov, Eur. Phys. J. C **74**, no. 7, 2942 (2014) [arXiv:1312.6486 [hep-ph]].
  - [18] V. Guzey, E. Kryshen and M. Zhalov, Phys. Rev. C **93**, no. 5, 055206 (2016) [arXiv:1602.01456 [nucl-th]].
  - [19] L. Frankfurt, M. Strikman, D. Treleani and C. Weiss, Phys. Rev. Lett. **101**, 202003 (2008) [arXiv:0808.0182 [hep-ph]].
  - [20] H. Mäntysaari and B. Schenke, Phys. Rev. Lett. **117**, no. 5, 052301 (2016) [arXiv:1603.04349 [hep-ph]].
  - [21] J. Breitweg *et al.* [ZEUS Collaboration], Eur. Phys. J. C **14**, 213 (2000) [hep-ex/9910038].
  - [22] R. M. Weber, DISS-ETH-16709, June 2006.
  - [23] F. D. Aaron *et al.* [H1 Collaboration], JHEP **1005** (2010) 032 [arXiv:0910.5831 [hep-ex]].
  - [24] S. R. Klein and J. Nystrand, Phys. Rev. Lett. **84**, 2330 (2000) [hep-ph/9909237].
  - [25] M. Strikman, M. Tverskoy and M. Zhalov, Phys. Lett. B **626**, 72 (2005) [hep-ph/0505023].
  - [26] Y. P. Ivanov, B. Z. Kopeliovich and I. Schmidt, arXiv:0706.1532 [hep-ph].
  - [27] V. P. Goncalves and M. V. T. Machado, Phys. Rev. C **84** (2011) 011902 [arXiv:1106.3036 [hep-ph]].
  - [28] G. Sampaio dos Santos and M. V. T. Machado, Phys. Rev. C **91** (2015) no.2, 025203 [arXiv:1407.4148 [hep-ph]].
  - [29] M. Klusek-Gawenda and A. Szczurek, EPJ Web Conf. **130** (2016) 05009 [arXiv:1609.04355 [hep-ph]].
  - [30] L. Adamczyk *et al.* [STAR Collaboration], Phys. Rev. C **96** (2017) no.5, 054904 [arXiv:1702.07705 [nucl-ex]].
  - [31] S. R. Klein, Nucl. Phys. A **967** (2017) 249 [arXiv:1704.04715 [nucl-ex]].